

# Structure–Function Relations in Molybdenum Sulfide Catalysts: The “Rim–Edge” Model

M. Daage and R. R. Chianelli<sup>1</sup>

Corporate Research Laboratories, Exxon Research and Engineering Company, Route 22 East, Annandale, New Jersey 08801

Received February 23, 1994; revised June 8, 1994

Chemical and physical studies of MoS<sub>2</sub> single crystals, microcrystals, and powders are carried out with the goal of understanding the relation between the morphology of the crystallites and their catalytic properties. Chemical etching of microcrystals is used to create new catalytic sites, which are responsible for the DBT (dibenzothiophene) hydrogenation reaction. Average stacking heights of poorly crystalline MoS<sub>2</sub> powders are then estimated by X-ray crystallography and for the first time correlated with the selectivity of the catalyst for hydrogenation versus HDS (hydrodesulfurization). This result is interpreted in terms of a simple physical model called the “rim–edge” model, where the catalyst particle can be described as a stack of several discs. The top and bottom discs are associated with the rim sites. The discs “sandwiched” between the top and bottom discs are associated with the edge sites. Sulfur hydrogenolysis is obtained on both the rim and edge sites, whereas the DBT hydrogenation occurs exclusively on the rim sites. A detailed kinetic analysis is used to model the variation in selectivity and to establish the turnover frequencies for the various reactions involved. © 1994 Academic Press, Inc.

## INTRODUCTION

For more than fifty years, molybdenum sulfide based catalysts have been used in hydroprocessing or hydroconverting feeds containing heteroatoms such as sulfur and nitrogen. Despite this widespread use, it is only relatively recently that the potential importance of “edge planes” which terminate the layered structure of MoS<sub>2</sub> has been recognized (1, 2). The importance of the “edges and corners” was first reported in the work of Voorhoeve *et al.* and Farragher *et al.* (3, 4). Experimental evidence for the role of these active surfaces comes from several physical catalytic studies on unsupported MoS<sub>2</sub>. For example, oxygen chemisorption (5), ESR (electron spin resonance) spin density (6), and magnetic susceptibility (7) have been correlated with the HDS (hydrodesulfurization) of DBT (dibenzothiophene) and associated with edge planes. Single crystal studies also showed the reactivity of the edge planes

toward olefin hydrogenation (8, 9) and their importance in the role of the cobalt promoters (10). Defects which are directly associated with sulfur vacancies as an essential part of the catalytic site are now well accepted (11, 12).

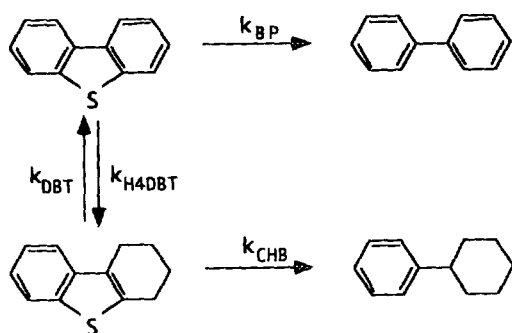
A recent paper reported that HDS activity also correlates with the optical defect density measured by PDS (photodeflection spectroscopy) (13). The quantitative association of the optically measured defects and the MoS<sub>2</sub> edge planes was established by performing the measurements on a series of single crystals, microcrystals, and microcrystalline powders. The PDS method now provides a direct method for measuring the edge-like defect site density in any MoS<sub>2</sub> catalyst. Furthermore, HDS rate measurements on microcrystallites whose edge area can be independently geometrically obtained led to the establishment of a fundamental turnover frequency for edge-like defects of  $7.9 \times 10^{-2}$  molecules/edge site·sec<sup>-1</sup> under the reaction conditions used. The establishment of this correlation now allows progress to be made in attacking more complex questions involving the role of the structure on the reactivity of MoS<sub>2</sub> catalysts. Such questions have already been addressed by several groups, but are generally limited to modeling of the catalyst activity in supported catalysts but with less work on unsupported systems (3, 14–22).

One such question is the effect that the structure has (if any) in determining the selectivity toward the pathways available in the HDS of DBT (Scheme 1). In this paper, we show that there is a direct connection between the degree of stacking of the MoS<sub>2</sub> layers as determined by X-ray diffraction and the selectivity toward hydrogenation of DBT. More precisely the existence of two types of sites, whose relative concentrations are stacking dependent, is proposed. A schematic of this model is indicated in Fig. 1. Turnover frequencies for the aromatic hydrogenation of DBT on “rim” sites and for HDS on rim and edge sites are given. Finally, the stacking dependence of the catalyst selectivity is quantitatively described.

## EXPERIMENTAL

*Preparation of microcrystals.* The microcrystals were grown by chemical vapor transport from MoS<sub>2</sub> powder

<sup>1</sup> To whom correspondence should be addressed.

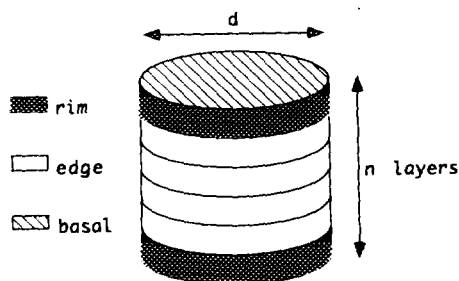
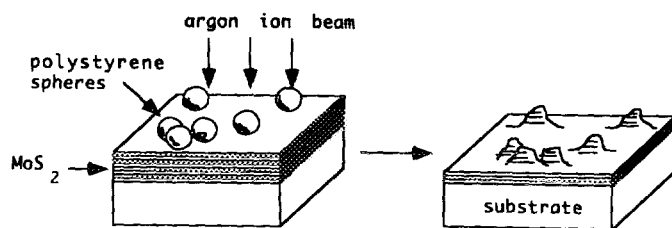


Scheme 1.

(Alpha Ventron reagent grade) as previously reported (11). The starting material was placed with an excess of sulfur in one end of a quartz tube which was then evacuated and sealed. That end of the tube was heated to 690°C while the opposite end was kept at 545°C. This process yielded small single crystals which were roughly hexagonal with diameters ( $\approx 1 \mu\text{m}$ ) 10 times larger than thickness (aspect ratio  $\sim 10:1$ ). Larger crystals (50–100  $\mu\text{m}$  diameter) were prepared for microscopy studies in the same way at 1050–1100°C. Oxidation of the crystals was carried out using water-saturated air at 590°C.

**Preparation of the powder.** The  $\text{MoS}_2$  powders were prepared by thermal decomposition of  $(\text{NH}_4)_2\text{MoS}_4$  in nitrogen at 250°C. The resulting  $\text{MoS}_3$  was then separated in batches and annealed in 15%  $\text{H}_2/\text{H}_2\text{S}$  for 2 hr at temperatures ranging from 350 to 900°C (12). High resolution microscopy of the materials showed that they had the "rag" structure and X-ray diffraction spectra characteristic of poorly crystalline  $\text{MoS}_2$ . Catalyst X-ray diffraction parameters as described below were determined after the catalytic runs. The Mo/S ratio after catalytic runs of this type are close to 1:2; however, small sulfur deficiencies are measured which are proportional to the edge area and this will be the subject of a future report.

**Preparation of single crystal edge surfaces.** As reported previously, synthetic edge surfaces can be pre-

FIG. 1. Rim/edge model of an  $\text{MoS}_2$  catalytic particle.FIG. 2. Lithographic preparation of  $\text{MoS}_2$  edge surfaces from a single crystal.

pared by lithographic methods from the basal plane of a single crystal (23). A thin film of  $\text{MoS}_2$  cleaved from a synthetic crystal is placed on a substrate so that the basal plane is exposed. A monolayer of monodisperse polystyrene spheres (0.2  $\mu\text{m}$  in diameter) is deposited onto the sample as an etching mask. The sample is then exposed to an argon ion beam (500 eV, 0.3  $\text{mA}/\text{cm}^2$ ) which removes the material between the spheres leaving  $\text{MoS}_2$  "posts" on the surface (Fig. 2). These synthetic edge surfaces have already been studied by XPS, PDS, and electron microscopy, and are ideal samples for the studies of the surface electronic structure, morphology, and chemical reactivity (23). In particular, the control afforded by lithographic processing allows the use of high resolution transmission microscopy.

**Catalytic tests.** The catalytic activity was determined using DBT as a model compound for hydrogenation and hydrodesulfurization. The reaction was carried out in a batch reactor designed to allow a constant hydrogen flow, according to the procedure already described (13). The operating conditions were: 1 to 2 g of catalyst, 100  $\text{cm}^3/\text{min}$  of hydrogen, 3000 kPa hydrogen, 350°C, 100  $\text{cm}^3$  of feed, and up to 7 hr contact times. The feed contained 0.4 wt% S as dibenzothiophene in a solvent of decalin (decahydronaphthalene). Product analysis was performed on a HP5880 gas chromatograph equipped with a 75% OV1-25% Carbowax 20 M fused silica column (50  $\text{m} \times 0.25 \text{ mm ID}$ ). The hydrodibenzothiophenes were identified by mass spectrometry.

**Kinetic analysis.** Four products are generally observed. According to the reaction pathway (Scheme 1), the two primary products are tetrahydrodibenzothiophene (H4DBT) and biphenyl (BP). Cyclohexylbenzene (CHB) is a secondary product and results from the desulfurization of the H4DBT. When BP was added to the feed, no conversion to CHB by direct hydrogenation was observed before all the sulfur has been removed. Traces of octahydro- and perhydrodibenzothiophene were detected by mass spectrometry. Because their concentrations were so low, no desulfurization products of these materials (likely bicyclohexyl) were detected. The results of the

measurements for the six catalysts used in this study are shown in Table 1.

For the desulfurization of DBT, Langmuir-Hinshelwood kinetics have been widely reported (24–26). According to the reaction pathway, described in Scheme 1, we obtain

$$-\frac{d[\text{DBT}]}{dt} = (k_{\text{BP}} + k_{\text{H4DBT}}) \frac{K_{\text{DBT}}[\text{DBT}]}{A} \times \frac{K_{\text{H}}P_{\text{H}}}{1 + K_{\text{H}}P_{\text{H}}} - k_{\text{DBT}} \frac{K_{\text{H4DBT}}[\text{H4DBT}]}{A} \quad [1]$$

$$-\frac{d[\text{H4DBT}]}{dt} = \left\{ k_{\text{CHB}} \frac{K_{\text{H4DBT}}[\text{H4DBT}]}{A} - k_{\text{H4DBT}} \frac{K_{\text{DBT}}[\text{DBT}]}{A} \right\} \times \frac{K_{\text{H}}P_{\text{H}}}{1 + K_{\text{H}}P_{\text{H}}} + k_{\text{DBT}} \frac{K_{\text{H4DBT}}[\text{H4DBT}]}{A} \quad [2]$$

$$-\frac{d[\text{BP}]}{dt} = -k_{\text{BP}} \frac{K_{\text{DBT}}[\text{DBT}]}{A} \times \frac{K_{\text{H}}P_{\text{H}}}{1 + K_{\text{H}}P_{\text{H}}} \quad [3]$$

$$-\frac{d[\text{CHB}]}{dt} = -k_{\text{CHB}} \frac{K_{\text{H4DBT}}[\text{H4DBT}]}{A} \times \frac{K_{\text{H}}P_{\text{H}}}{1 + K_{\text{H}}P_{\text{H}}}, \quad [4]$$

where

$$A = 1 + K_{\text{DBT}}[\text{DBT}] + K_{\text{H4DBT}}[\text{H4DBT}] + K_{\text{CHB}}[\text{CHB}] + K_{\text{BP}}[\text{BP}] + K_{\text{H}_2\text{S}}[\text{H}_2\text{S}],$$

$K_i$  and  $[i]$  are the adsorption constant and concentration of species  $i$ ,  $k_i$  are the rate constants, and  $P_{\text{H}}$  is the pressure of hydrogen.

Under the experimental conditions used in this study, several simplifications can be applied based on the following:

—The hydrogen pressure term is constant and can be included in the rate constant (strictly speaking this assumption is not correct if the hydrogen pressure is not constant and different hydrogen pressure dependencies could occur in Eqs. [1]–[4].

—The inhibition due to  $\text{H}_2\text{S}$  is not significant because of the constant hydrogen sweeping.

—The inhibition terms due to biphenyl and cyclohexylbenzene can be neglected because no inhibition of the desulfurization reaction was observed when either BP or CHB were added to the feed.

—The unity in the denominator can also be neglected

TABLE 1

Products of the Desulfurization of DBT as a Function of Time for  $\text{MoS}_2$  Catalysts Prepared at Various Temperatures

Time (hr)	CHB (%)	BP (%)	H4DBT (%)	DBT (%)
a: 350°C				
1.0	0.1	1.1	2.5	96.3
1.5	0.2	3.9	6.5	89.4
2.0	2.3	6.5	8.5	82.7
3.0	6.8	11.6	9.5	72.1
4.0	11.3	16.7	8.9	63.1
5.0	15.0	21.7	7.8	55.5
6.0	20.9	26.7	6.6	45.8
7.0	25.2	31.8	5.4	37.6
b: 450°C				
1.0	0.1	1.5	2.8	95.6
1.5	0.9	4.0	6.0	89.1
2.0	2.1	6.5	8.0	83.4
3.0	5.5	10.7	9.8	74.0
4.0	8.5	15.5	8.6	67.4
5.0	12.4	20.7	8.0	58.9
6.0	17.0	24.3	7.4	51.3
7.0	20.4	29.0	6.0	44.6
c: 550°C				
1.0	0.1	1.3	2.3	96.3
1.5	0.5	3.6	5.1	90.8
2.0	1.6	5.3	6.9	86.2
3.0	4.3	9.6	8.3	77.8
3.5	5.2	11.8	8.8	74.2
4.5	8.6	15.8	8.3	67.3
5.0	10.6	17.3	8.2	63.9
6.0	13.6	21.5	7.3	57.6
7.0	16.7	25.6	6.8	50.9
d: 650°C				
1.0	0.2	0.8	0.8	98.2
1.5	0.2	2.9	2.5	94.4
2.0	0.8	4.5	3.9	90.8
3.0	2.2	8.7	5.1	84.0
4.0	3.5	12.7	6.1	77.7
5.0	5.9	15.6	6.1	72.4
6.0	8.2	19.7	6.3	65.8
7.0	10.1	23.5	5.9	60.5
e: 750°C				
1.0	0.1	0.7	0.5	98.7
1.5	0.1	2.6	1.7	95.6
2.0	0.4	4.0	2.4	93.2
3.0	1.3	7.6	4.2	86.9
4.0	2.4	11.2	4.8	81.6
5.0	4.2	14.5	5.3	76.0
6.0	5.6	17.2	5.0	72.2
7.0	7.4	20.8	5.1	66.7
f: 900°C				
1.0	0	0.4	0.2	99.4
1.5	0	1.0	0.5	98.5
2.0	0	1.8	0.8	97.4
3.0	0.1	3.1	1.5	95.3
4.0	0.3	4.1	1.9	93.7
5.0	0.4	5.8	2.5	91.3
6.0	0.7	6.6	2.5	90.2
7.0	0.9	8.3	3.0	87.8

because initial rates were found to be independent of the DBT concentration (0.2 to 0.8 wt% S range) suggesting that  $K_{\text{DBT}} \cdot [\text{DBT}] \gg 1$ . Such approximation is consistent with the data reported by Singhal *et al.* (24).

—Because of the low concentration of H4DBT, the precision obtained in the kinetic modeling did not justify the use of two different adsorption constants for DBT and H4DBT.

Based on the above approximations, the following set of equations has been used and solved with a Runge–Kutta method (27):

$$-\frac{d[\text{DBT}]}{dt} = (k_{\text{BP}} + k_{\text{H4DBT}}) \frac{[\text{DBT}]}{[\text{DBT}] + [\text{H4DBT}]} - k_{\text{DBT}} \frac{[\text{H4DBT}]}{[\text{DBT}] + [\text{H4DBT}]} \quad [5]$$

$$-\frac{d[\text{H4DBT}]}{dt} = -k_{\text{H4DBT}} \frac{[\text{DBT}]}{[\text{DBT}] + [\text{H4DBT}]} + (k_{\text{CHB}} + k_{\text{DBT}}) \frac{[\text{H4DBT}]}{[\text{DBT}] + [\text{H4DBT}]} \quad [6]$$

$$-\frac{d[\text{BP}]}{dt} = -k_{\text{BP}} \frac{[\text{DBT}]}{[\text{DBT}] + [\text{H4DBT}]} \quad [7]$$

$$-\frac{d[\text{CHB}]}{dt} = -k_{\text{CHB}} \frac{[\text{H4DBT}]}{[\text{DBT}] + [\text{H4DBT}]} \quad [8]$$

In addition, the excess of hydrogen consumption during the hydrodesulfurization, which is due to the aromatic ring hydrogenation, can be expressed by the selectivity between the production of the BP and the CHB. In that case, apparent zero order rate constants are used and correspond to the slopes of the conversion versus time plots for the corresponding molecules. These rate constants (noted  $k_x^*$  in the text) are in fact equal to the product of the real rate constant ( $k_x$ ) by the ratio H4DBT/(H4DBT + DBT) for the CHB or DBT/(H4DBT + DBT) for the BP at steady-state conditions.

The turnover frequencies are calculated by assuming that the rate constants correspond to the product of the turnover frequency ( $\alpha$ ) times the site density (HYD or HDS). Note that the turnover frequency includes the turnover number as well as the exponential term due to the activation energy. Therefore, the turnover frequencies reported here are only valid for a reaction temperature of 350°C.

## RESULTS

The major finding of this paper is that a relation between the morphology and the catalytic selectivity of edge surfaces of MoS<sub>2</sub> single crystals can be demonstrated from

the data. As was previously observed (13), microcrystalline MoS<sub>2</sub> catalyzes the hydrodesulfurization of DBT but not its hydrogenation. This is in stark contrast to disordered powders, which exhibit both reactions in varying degrees. The high selectivity (>200) of the microcrystals can be destroyed by chemical etching of the surface. Figure 3 shows transmission electron micrographs (TEM) of lithographically prepared MoS<sub>2</sub> edge surfaces. The material on the left is not etched and shows the individual layers 6 Å apart terminating in a smooth edge surface. This sample was then treated in HCl vapor for 2 hr at 200°C, resulting in the surface shown on the right side of Fig. 3. A roughened surface is obtained with the formation of steps 3 to 10 layers high. When a similar treatment is applied to microcrystalline MoS<sub>2</sub>, the optical absorption changes as illustrated by the PDS measurement (Fig. 4). Since the optical defect density has been correlated with the HDS activity (13), the change observed reflects a change in the catalytic performance. Table 2 shows the activities observed on such microcrystals. The HCl treatment induces the formation of H4DBT as a product, strongly suggesting that the hydrogenation reaction occurs on a different site, which may be associated with the steps shown in Fig. 3, and that PDS measures both the HDS sites and the hydrogenation sites (HYD). Such hydrogenation sites can also be introduced using oxygen as etching agent. Figure 5 shows scanning electron micrographs (SEM) of a large MoS<sub>2</sub> crystal before and after treatment with air. The same sort of surface roughening is observed, although on a much larger scale. The hydrogenation activity of these microcrystals is also dramatically increased by this treatment (Table 2). In addition, when poorly crystalline powders containing chlorine or oxygen were used, the desulfurization reaction induces a resulfiding of the surface and no chlorine or oxygen remained in the catalysts recovered at the end of run. This shows in particular that the increased hydrogenation is not related to the specific chemical used for the etching (influence of residual chlorine for example), but rather to the morphological change which introduces the hydrogenation sites. We propose a specific model to explain all of the observed kinetic data described below which were designed to test this idea.

The model proposed is that the selectivity of the HDS of DBT is dependent on the ratio of number of layers with exposed basal planes to the number of layers which have basal planes covered by adjacent layers of MoS<sub>2</sub>. Sites located near the edge of the former layers are called rim sites and those at the edge of the latter are called edge sites. This is illustrated schematically in Fig. 1. To test this idea catalysts were prepared for which the crystalline order along both the a-axis (parallel to the basal plane) and c-axis (perpendicular to the basal plane) were known and varied over a wide range. This was achieved by using

## HCl TREATMENT INTRODUCES 'RIM' SITES

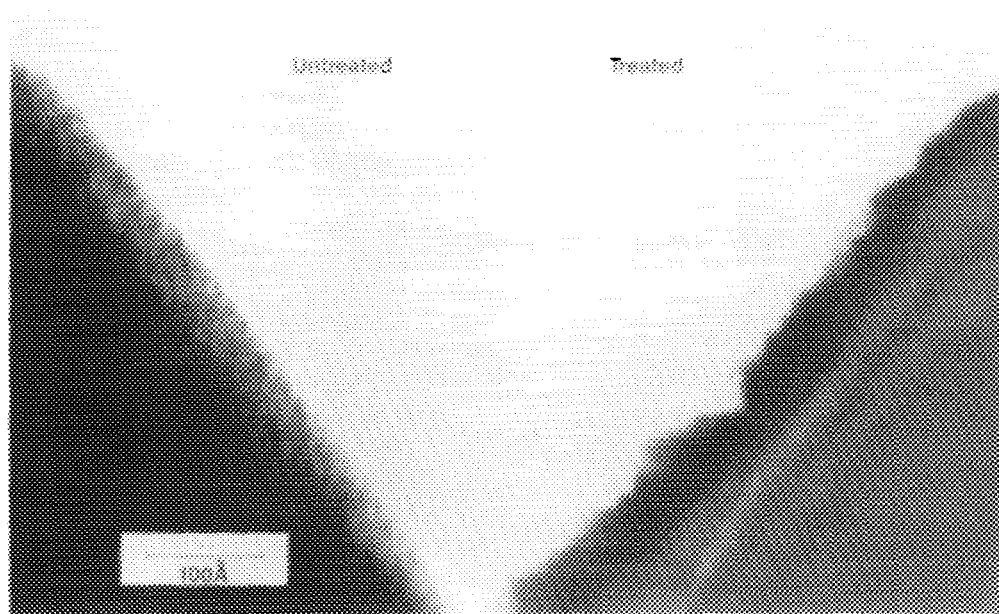


FIG. 3. TEM of lithographically prepared  $\text{MoS}_2$  edge surfaces: (a) untreated surface, (b) HCl treated surface.

a set of poorly crystalline powders annealed at different temperatures as described above. From these catalysts it was also possible to obtain an estimate of the relative site densities of each type of site.

*Activity and morphology of poorly crystalline  $\text{MoS}_2$  catalysts.* Poorly crystalline powders are prepared by heating amorphous  $\text{MoS}_3$  in a sulfiding atmosphere. This heating causes a partial crystallization in a structure previously termed the rag structure (11). The rag consists of

several stacked, but highly folded and disordered  $\text{MoS}_2$  layers. Although only 20 to 100 Å thick in the stack direction, the layers extend several thousand Å perpendicularly to the *c*-axis. By varying the preparation conditions, such as the annealing temperature, one can vary the stacking height as well as the diameter of the layers. Figure 6 illustrates the typical X-rays diffraction patterns of a set of poorly crystalline  $\text{MoS}_2$  powders obtained at various anneal temperatures. These spectra exhibit a strong 002 peak in the low angle region and a broad envelope between  $2\theta = 30^\circ$  to  $2\theta = 60^\circ$ . This envelope contains numerous reflections with well-defined maxima for the 100, 103, and 110 reflections. The 103 maximum indicates that the 2H (two layer hexagonal) molybdenite stacking sequence is retained in the crystallites. The asymmetric shape of the 100 is characteristic of random layer lattice structures in which the layers are displaced with respect to each other (11). The shape of the 002 diffraction peak, however, is relatively insensitive to random layer lattice structures. The dimension of the particles along the *c*-axis is therefore very similar to the crystalline order and can be directly estimated from the width of the 002 line. From the narrowing of the 002 peak, it is clear that the higher temperatures increase the crystalline order along the *c*-axis, which corresponds to an apparent average stacking height (*h*). After correction of the 002 width from the instrumental broadening, *h* can be estimated using the Debye-Scherrer equation:  $h = k\lambda / (2 \cos \cdot \Delta\theta)$  with  $\Delta\theta = (\Delta\theta_{\text{measured}} -$

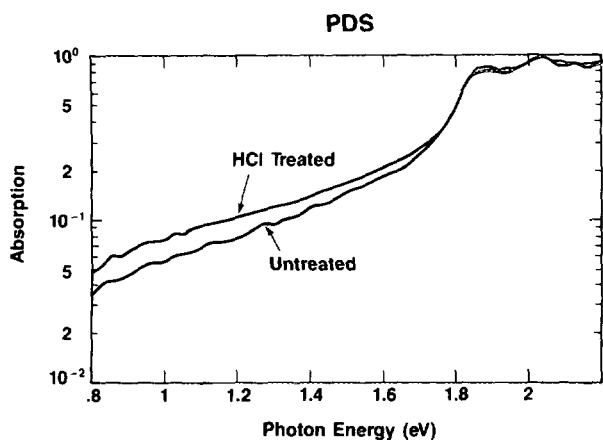


FIG. 4. Optical adsorption of synthetic edge surfaces shown in Fig. 3 (13).

TABLE 2  
Activities of MoS<sub>2</sub> Microcrystals for  
the HDS and Hydrogenation of DBT

MoS <sub>2</sub> platelets	BP <sup>a</sup>	HDBT <sup>a</sup>
Untreated	5.3	0
Oxygen treated	7.8	0.7
HCl treated	6.5	0.4

<sup>a</sup> 10<sup>16</sup> molecules/g · s.

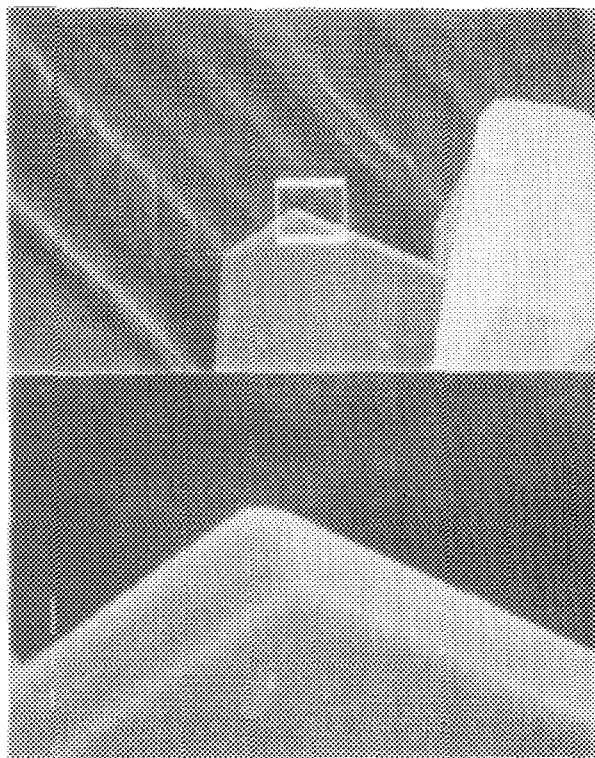
$b$ ),  $b \approx 0.2^\circ 2\theta$ ,  $\lambda = 1.5414 \text{ \AA}$ , and a shape factor  $k = 0.76(11)$ . The apparent average number of layers reported in Table 3 were calculated using  $n = h/6.17$  ( $h$  in  $\text{\AA}$ ).

The particle size along the basal plane cannot be measured from the X-ray spectra in a similar manner because of the folding of the layers and only the crystalline order along the basal plane can be estimated by using the widening of the 110 diffraction peak. For samples prepared below 750°C the observed crystalline order lengths ( $L$ ) are 43, 47, 50, and 59  $\text{\AA}$ . This variation is quite small compared to the change observed for the stacking (19 to 44  $\text{\AA}$ ) in the same temperature region. In fact, the ratio

$h/L$  is not constant and reflects that the crystallization is anisotropic. Moreover, the large decreases in the intensity ratios ( $I_{103}/I_{002}$  and  $I_{110}/I_{002}$ ) clearly confirm that stacking is the parameter the most affected by the annealing temperature. Thus, crystalline order is introduced more quickly in the stack direction as the samples are annealed than within the layer and considerable disorder still remains even at the highest temperature.

*Hydrodesulfurization of dibenzothiophene.* The HDS rate constants for these materials are reported in Table 4. Each of the rate constants decreases as the MoS<sub>2</sub> becomes more crystalline. However, a 36-fold variation is observed for the formation of the H4DBT whereas only a 8-fold variation occurs for the production of desulfurized products (BP, CHB). Consequently, large variations in the selectivities of the reaction are observed. These variations are related to the stacking of the layers, as it is particularly illustrated by Fig. 7, which shows that the ratio  $S_1 = k_{\text{H4DBT}}/k_{\text{BP}}$  is linearly correlated with the reciprocal of the apparent average number of layers stacked. In Fig. 7, we also included one data point for the microcrystals which have negligibly small  $k_{\text{H4DBT}}$  and a  $\Delta\theta$  so small that it is instrumentally broadened. By contrast, a more complicated relation is observed for the selectivity  $S_2 = k \cdot \text{CHB}/$

Untreated



Oxygen treated

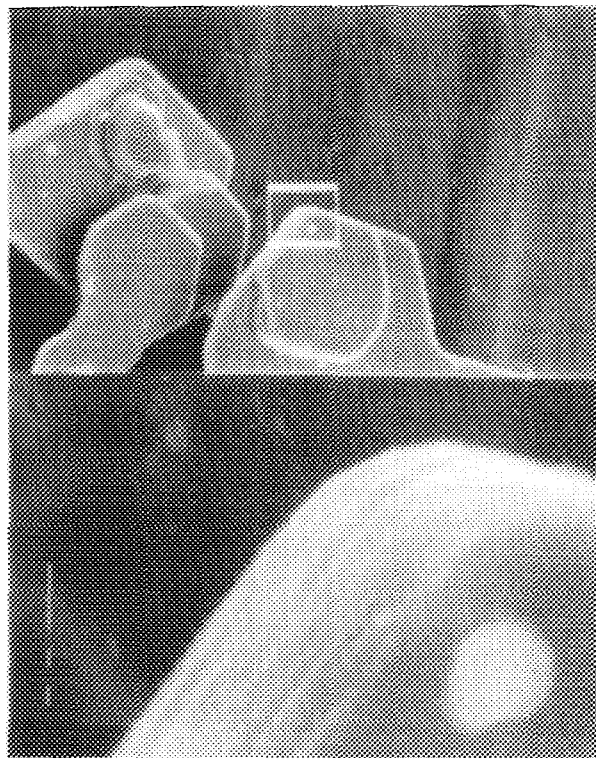


FIG. 5. SEM of MoS<sub>2</sub> microcrystals: a) untreated crystallites, b) Oxygen treated crystallites (small marks are 1 $\mu$ ).

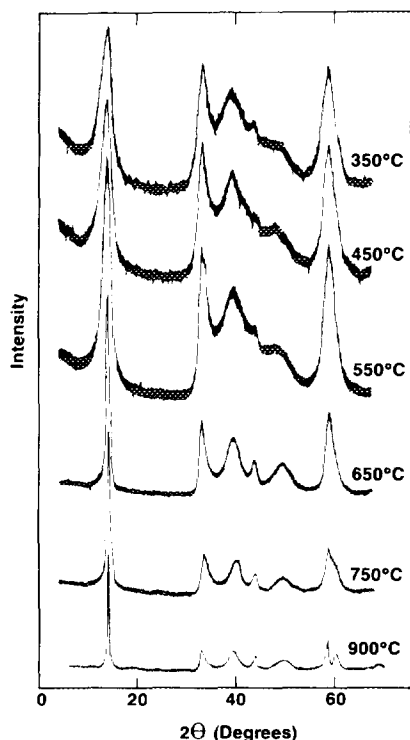


FIG. 6. X-ray diffraction patterns of MoS<sub>2</sub> poorly crystalline powders annealed at different temperatures.

( $k^*_{BP} + k^*_{CHB}$ ) as seen in Fig. 8. This has to be expected since secondary reactions are involved in the formation of CHB. Also, the ratio H4DBT/DBT approaches a constant value ( $\rho$  in Table 4) which depends on the anneal temperature of the catalyst as can be seen in Fig. 9. Because an equilibrium is only dependent on the reaction conditions, one must conclude that this constant value is due to a steady-state kinetic regime. The variation of the ratio [H4DBT]/[DBT] with the anneal temperature should

TABLE 3

Apparent Average Stacking Heights of MoS<sub>2</sub> Formed at Various Temperatures

$T$ (°C)	$\Delta_{002}$ (degrees)	$h$ (Å)	$n$ (layer)
350	2.64	19.0	3.1
450	2.53	20.9	3.4
550	2.24	23.4	3.8
650	1.20	44.0	7.1
750	0.84	62.0	10.1
900	0.56	93.5	15.2

TABLE 4

Rate Constants for the DBT Reactions on MoS<sub>2</sub> Powders

$T$ (°C)	$k_{BP}$	$k_{H4DBT}$	$k_{DBT}$	$k_{CHB}$	$\rho^b$	$k^*_{CHB}$
350	12.0	29.0	147.0	77.0	0.142	10.9
450	10.7	23.1	120.0	67.4	0.136	9.2
550	6.2	12.1	62.0	40.0	0.131	5.2
650	5.6	5.9	30.0	37.0	0.098	3.6
750	3.7	2.9	13.6	26.0	0.078	2.0
900	1.5	0.8	4.0	9.0	0.054 <sup>c</sup>	0.5

Note. Rate constants in  $10^{16}$  molecules  $\cdot$  g<sup>-1</sup>  $\cdot$  s<sup>-1</sup>.

<sup>b</sup> Experimental H4DBT/DBT ratio.  
<sup>c</sup> Calculated from the kinetic model.

therefore be related to different variations of the concentrations of two distinct sites.

*The origin of the selectivity/stacking relationship.* We have described a model above, which assumes that the catalyst particles are made of a stack of  $n$  discs and of diameter  $d$  (Fig. 1). The top and bottom layers have sites occurring at their edges called rim sites while layers "sandwiched" in the middle have only edge sites. The top surface of the disc away from the edge is the inert basal plane. Stereochemical bonding considerations described below suggest that the hydrogenation reaction is more constrained than the hydrogenolysis in the HDS reaction and that only sites which allow the proper interaction of the reacting molecule with the site can allow the formation of the tetrahydrodibenzothiophene, whereas sites with

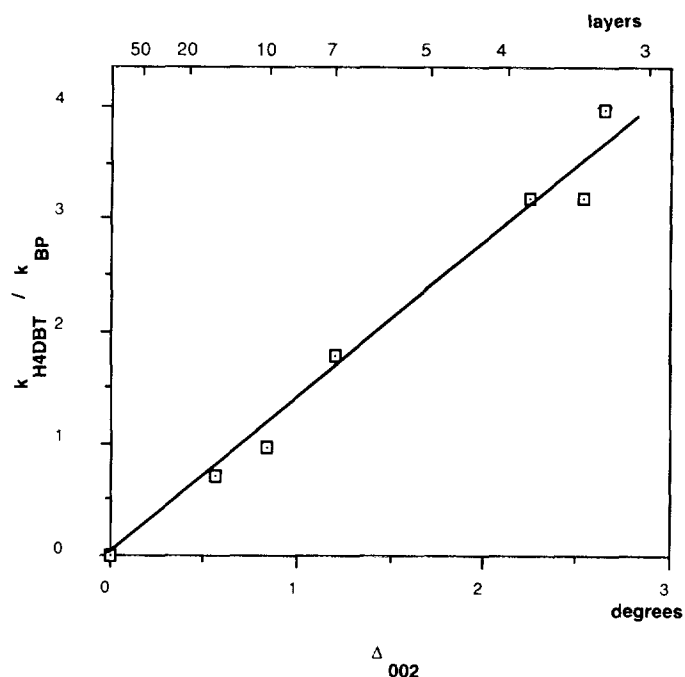


FIG. 7. Stacking dependence of the selectivity  $S_1$ .

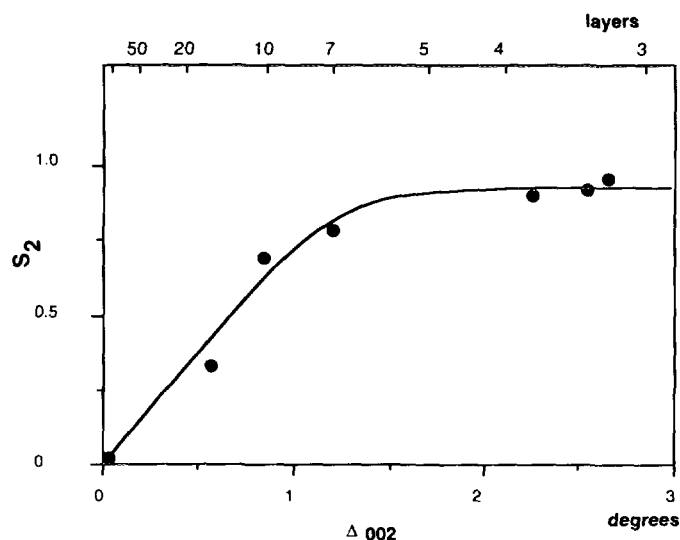


FIG. 8. Stacking dependence of the selectivity  $S_2$ .

fewer interaction constraints catalyze the HDS reaction. Literature cited above dealing with two sites generally call the hydrogenation sites "corner sites" reflecting a higher unsaturation (usually three missing sulfur atoms), and the HDS sites are called edge sites reflecting a lower unsaturation (usually one missing sulfur atom). We propose in this paper that the hydrogenation of DBT occurs on rim sites which occur only on the rim and also permit the proper interaction of the molecule with the catalytic sites. We do not consider further division of the rim sites into "rim corner and rim edge sites" in this report.

Consequently, rim sites dominate the hydrogenation and the selectivity for hydrogenation should be related to the ratio rim to edge sites. In order to proceed, we will consider two models representing the extreme cases which include the corner sites. The first model, which we will call the "rim-edge" model, assumes that the hydrogenation occurs exclusively on rim sites. In that case, the corners are considered edges or rim sites depending on which layer they are located. In the second model, the hydrogenation is associated with the corner sites and all the layers are chemically independent of each other and behave in an identical manner. This model will be called the "corner-edge" model. Note that the geometric model described by Kasztelan represents a particular case of the corner-edge model since the number of corners is fixed at six for hexagonal particle (20).

From Fig. 7 it was seen that the selectivity  $S_1$  varies linearly with the reciprocal of the average stacking. Such a correlation is straightforward when the rim-edge model is used. For this model, the relative density of rim and edge sites is

$$\frac{r}{r+e} = \frac{2\pi d}{\pi dn} = \frac{2}{n}, \quad [9]$$

where  $r$  is the number of rim sites and  $e$  the number of edge sites. It is important to note that this relative density does not depend upon the particle diameter or shape, but only on the stacking. When using the corner-edge model, the correlation is less obvious. The data clearly indicate that the selectivity can be predicted by knowing the stack height of the  $\text{MoS}_2$  stack height and strongly suggests that for the DBT test reaction the sites which predominate on the rims and edges are distinct. Later we shall return to the discussion regarding corner sites and the selectivity of single layers.

*Site densities and turnover frequencies on poorly crystalline  $\text{MoS}_2$ .* As described above, only BP was formed on the surfaces of geometrically well-defined microcrystalline  $\text{MoS}_2$ . Microcrystalline  $\text{MoS}_2$  is geometrically well defined because edge areas of collections of microcrystals can be measured directly using electron microscopy. Rates can then be measured on these collections of microplatelets and a turnover frequency determined for the conditions measured. Using this method, a turnover frequency of  $7.9 \times 10^{-2}$  molecules of DBT  $\cdot$  site $^{-1} \cdot$  sec $^{-1}$  was determined for  $\text{MoS}_2$  edge planes operating under catalytic conditions identical to those used in this paper (13). This turnover frequency  $\alpha_{\text{BP}}$  now becomes a fundamental input to calculating properties of the geometrically undefined powders. The powders are geometrically undefined because, while we do have their stacking heights defined, we do not have knowledge of the total edge area or "diameter" of the  $\text{MoS}_2$  sheets except through the activity measurements. In the next section, we use  $\alpha_{\text{BP}}$  determined from the microcrystallites and the X-ray diffraction data described above to further model the relationship between the physical properties of the  $\text{MoS}_2$  catalyst and its selectivity in DBT desulfurization.

We illustrate using two hypotheses, with others being eliminated through inconsistencies with the observed microplatelet results. In hypothesis A, we assume that the BP is produced on both HYD and HDS sites (on both rim and edge sites). According to the rim-edge model described above, the total site densities (rim + edge) are calculated from the BP rate constant reported in Table 4 by dividing them by  $\alpha_{\text{BP}}$ . The results are shown in Table 5 and illustrated in Fig. 10. Also for the rim-edge model, the relative proportion of rim to (rim + edge) equals  $2/n$  (Eq. [9]) above. Table 5 reports the values of  $r$ ,  $(r+e)$  and  $e$  obtained by using this ratio applied to the previously calculated BP site density. Now for any given reaction, a linear correlation including the origin should be obtained between the concentration of the catalytic site and the activity. From the slope of such plots, turnover frequen-



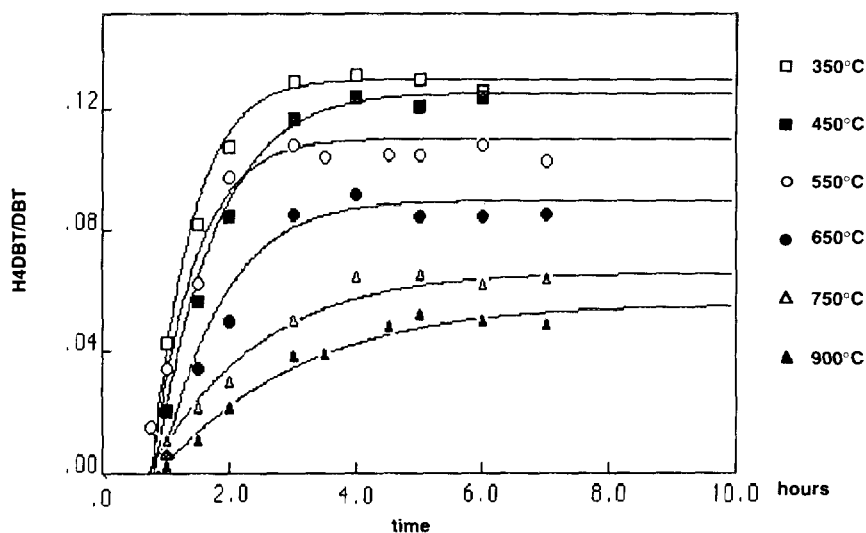


FIG. 9. Variation of H4DBT/DBT ratio vs time for catalysts annealed at different temperatures.

cies can be extracted. This is illustrated in Fig. 11 for the formation of the H4DBT and a turnover frequency of  $0.291 \text{ molecules} \cdot (\text{rim site})^{-1} \cdot \text{s}^{-1}$  is found. For the dehydrogenation of the H4DBT to form the DBT a similar relationship exists and is shown in Fig. 12. The turnover frequency is  $1.45 \text{ molecules} \cdot (\text{rim site})^{-1} \cdot \text{s}^{-1}$ . If the edge or edge + rim site concentrations are used for hydrogenation, a linear correlation may be obtained, but will not include the origin. This shows unambiguously that the dehydrogenation occurs only on the rim sites, which is consistent with the principle of the microreversibility. For the formation of CHB a similar correlation is obtained when the (rim + edge) site concentration is considered. The corresponding turnover frequency is  $0.486 \text{ molecules} \cdot (\text{rim} + \text{edge site})^{-1} \cdot \text{s}^{-1}$  as indicated in Fig. 13. Like the desulfurization of DBT to BP, this reaction corresponds to a desulfurization process and takes place on both rim and edge sites.

The relationship between the selectivity  $S_2$  and the apparent stacking  $n$ . As illustrated in Fig. 8, the selectivity  $S_2$  was related to the stacking of the  $\text{MoS}_2$  layers, but no linear relationship was found. It is noteworthy that the rim-edge model provides a better understanding of this relationship. The selectivity  $S_2$  is defined by

$$S_2 = \frac{k_{\text{CHB}}^*}{k_{\text{CHB}}^* + k_{\text{BP}}^*} = \frac{1}{1 + k_{\text{BP}}^*/k_{\text{CHB}}^*} \quad [10]$$

replacing  $k_x^*$  by their expressions for the rim-edge model, gives

$$S_2 = 1 / \left[ 1 + \frac{\alpha_{\text{BP}}(r + e) \frac{\text{DBT}}{\text{H4DBT} + \text{DBT}}}{\alpha_{\text{CHB}}(r + e) \frac{\text{H4DBT}}{\text{H4DBT} + \text{DBT}}} \right], \quad [11]$$

TABLE 5  
Site Densities for Hypotheses A and B

$T$ ( $^{\circ}\text{C}$ )	$\frac{r}{r+e} = \frac{2}{n}$	Hypothesis A			Hypothesis B		
		$r$	$e$	$r+e$	$r$	$e$	$r+e$
350	0.645	98.0	54.0	152.0	276.2	152.0	428.2
450	0.588	79.6	55.8	135.4	193.2	135.4	328.6
550	0.526	41.3	37.2	78.5	88.2	78.5	166.7
650	0.282	20.0	50.9	70.9	27.8	70.9	98.7
750	0.198	9.3	37.5	46.8	11.6	46.8	58.4
900	0.132	2.5	16.5	19.0	3.3	19.0	22.3

Note. Sites densities in  $10^{16} \text{ sites} \cdot \text{g}^{-1}$ .

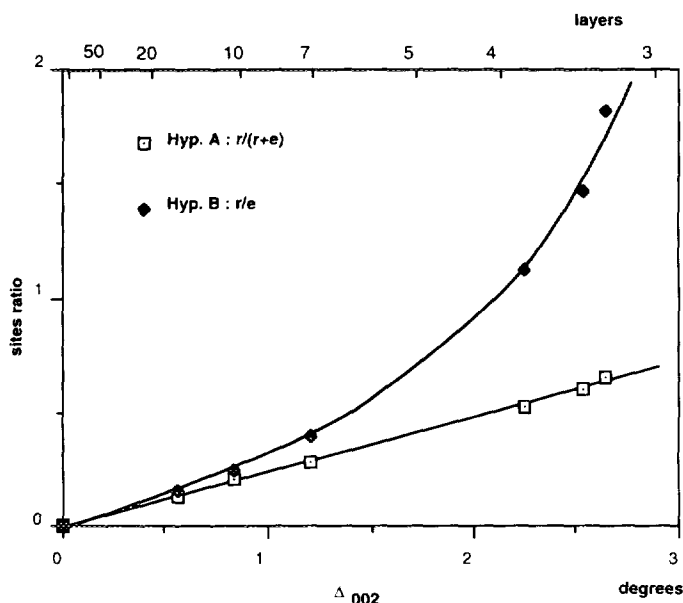


FIG. 10. Relation between the sites ratio and the width of the 002 diffraction peak for hypothesis A and B.

where  $\alpha_i$  and  $(r + e)$  are the turnover frequencies and the (rim + edge) site density.

After simplification, we obtain

$$S_2 = \frac{1}{1 + \frac{\alpha_{BP}}{\alpha_{CHB}} \frac{DBT}{H4DBT}} = \frac{1}{1 + \frac{\alpha_{BP}}{\alpha_{CHB}} \cdot \frac{1}{\rho}} \quad [12]$$

It then appears that the selectivity is directly dependent on the ratio  $\rho$  ( $\rho = H4DBT/DBT$ ). As mentioned above this ratio reaches a constant value. This result denotes the existence of a steady state for our reaction conditions, which is described by

$$\frac{d([H4DBT])/[DBT]}{dt} = \frac{1}{[DBT]^2} \left( \frac{d[H4DBT]}{dt} \cdot [DBT] - [H4DBT] \cdot \frac{d[DBT]}{dt} \right) = 0, \quad [13]$$

applying Eqs. [5] and [6],

$$-k_{DBT} \frac{[H4DBT]^2}{[DBT]^2} + (k_{BP} + k_{H4DBT} - k_{DBT} - k_{CHB}) \frac{[H4DBT]}{[DBT]} + k_{H4DBT} = 0. \quad [14]$$

For the rim-edge model, it becomes

$$\alpha_{H4DBT} + [(\alpha_{BP} - \alpha_{CHB}) \frac{n}{2} + (\alpha_{H4DBT} - \alpha_{DBT})] \rho - \alpha_{DBT} \rho^2 = 0, \quad [15]$$

where  $n$  is the apparent stacking, and  $\alpha_i$  are the turnover frequencies.

For our set of experiments, we have

$$\rho^2 + (0.14n + 0.80)\rho - 0.20 = 0. \quad [16]$$

In Fig. 14, the experimental values of  $S_2$  are compared with the calculated values obtained from Eq. [16] and the apparent stacking  $n$  determined by X-rays. In general, the calculated values are slightly higher, but in reasonable agreement.

In first approximation, the term  $\rho^2$  can be neglected in Eqs. [15] and [16] when  $\rho$  is small as in our results. Then

$$\rho \approx \frac{\alpha_{H4DBT}}{(\alpha_{CHB} - \alpha_{BP})(n/2) + (\alpha_{DBT} - \alpha_{H4DBT})} \approx \frac{1}{0.70n + 3.98}, \quad [17]$$

applying Eq. [17] to Eq. [12],

$$S_2 = \frac{1}{\left( \frac{\alpha_{BP}}{\alpha_{CHB} \cdot \alpha_{H4DBT}} \left[ (1 + \alpha_{DBT} - \alpha_{H4DBT}) + (\alpha_{CHB} - \alpha_{BP}) \frac{n}{2} \right] \right)}, \quad [18]$$

and

$$S_2 = \frac{1}{0.114n + 1.645}. \quad [19]$$

Therefore, it appears that there is a simple correlation between the selectivity  $S_2$  and the apparent stacking. Figure 14 shows the variation of  $S_2$  with the apparent stacking using Eq. [19] and a good agreement with the experimental data is observed.

## DISCUSSION

It has generally been observed that the basal planes of  $MoS_2$  catalysts are inert to adsorption of reacting molecules. However, reactions which are dependent on basal plane activity have been reported. The most striking example comes from the work of Tanaka *et al.* who demonstrated using model compounds that hydrocarbon isomerization occurs on the basal plane and that hydrogen transfer occurs on edge planes (28). This was done by measuring the activity of a single crystal for two model reactions, then cutting the same crystal into pieces, thus increasing the edge area while essentially keeping the

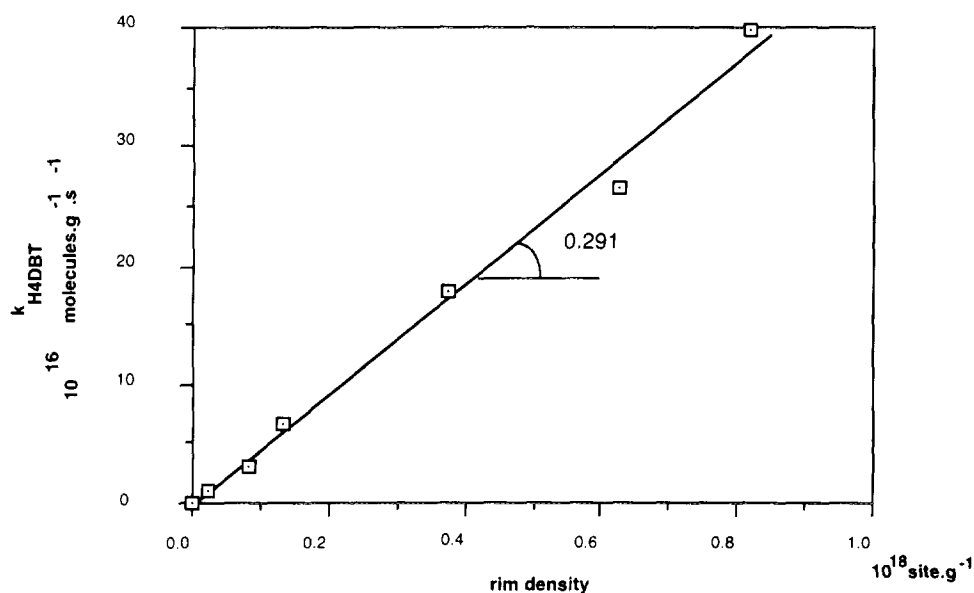


FIG. 11. Turnover frequency of rim sites for DBT hydrogenation.

basal plane area constant. Applying the language of this report, Tanaka varied the rim to edge ratio of the sites making it unnecessary to invoke the hydrogenation activity of the basal plane itself. It was also reported by Kemp *et al.* that stacking determined the selectivity in a group of hydrotreating catalysts (29).

Because of the inertness of the basal plane and the clearly demonstrated importance of the edge area for total activity, the importance of the stack height of  $\text{MoS}_2$  catalysts has largely been overlooked. Most workers, such

as Kastelan *et al.*, studied supported catalysts which are generally single layers and have low stack number but did not vary the stacking height of the catalysts (20). Where unsupported catalysts were studied, such as in the work of Voorhoeve *et al.*, the stack was also not varied in a systematic manner (3).

Much of the work cited above has been accomplished regarding the selectivity of the HDS reaction. It is generally accepted that the catalytic activity is closely associated with the edges of the layers and that two sites are

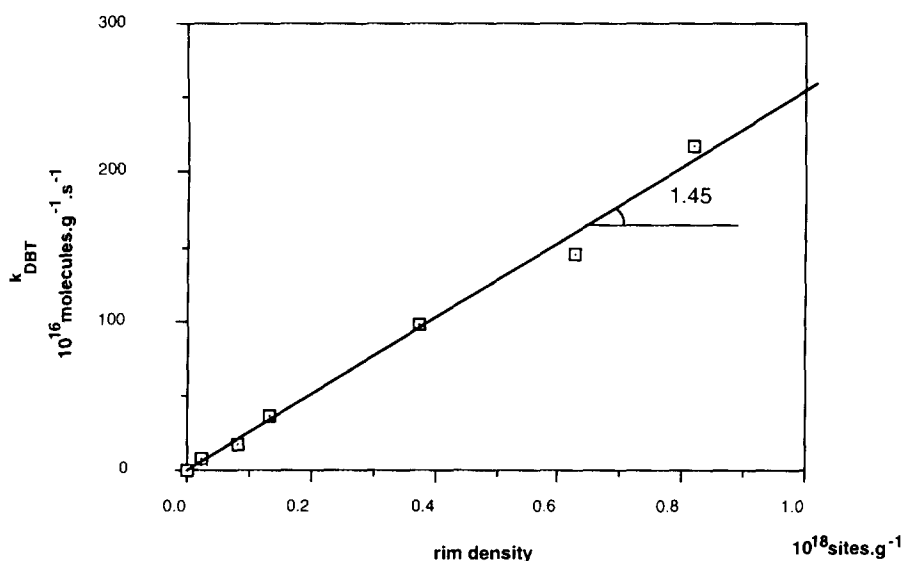


FIG. 12. Turnover frequency of rim sites for dehydrogenation of H4DBT.

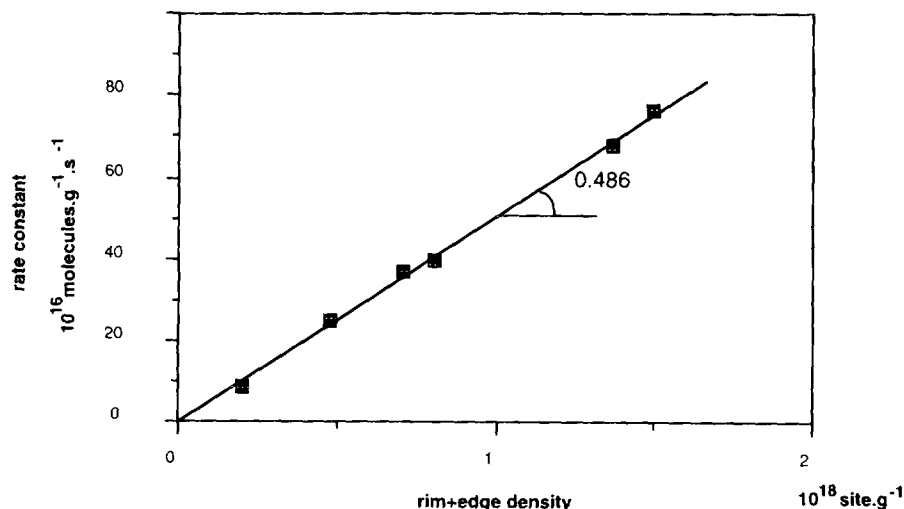


FIG. 13. Turnover frequency of HDS sites for desulfurization of H4DBT.

involved. Sulfur vacancies, which are critical for the adsorption of an organic molecule, occur more readily on the edge because the sulfur atoms are either bonded to one or two molybdenum ions. Such structures are more reducible than the triply bonded form, which exists on the basal plane. Previous models correlate the activity for HDS and hydrogenation with these particular structures. Massoth *et al.* suggested that HDS reactions occur on corner sites and hydrogenation reactions on edge sites (14), whereas Kasztelan *et al.* concluded that both reactions occurred on the edge sites (22). Again these models were generally derived from studies in which the stacking height was not varied based on the assumption that each layer of molybdenum disulfide is chemically independent

of each other because their stacking is strictly due to Van der Waals interactions.

Another important feature of the earlier studies is that they were usually done using thiophene as a model compound. In fact, that is one of the constraints of the work that was highlighted by Kasztelan *et al.* (22). This study used DBT and it is likely that the effects described in this report are only important for larger molecules where steric hindrance is important. DBT is a large molecule that can cover an area as large as  $8.0 \times 12.2 \text{ \AA}^2$  in a flat adsorption mode. Such an area is much larger than a single Mo site and steric hindrances with the neighboring molybdenum atoms in the same layer as well as the next layer have to be expected. It is this aspect of the rim site vs the edge site which we wish to emphasize in this report. Previous models generally did not consider these steric effects in larger molecules, but emphasized the stereochemical adsorption of aromatics and thiophene on coordinatively unsaturated sites.

This may be illustrated by considering the possible modes of adsorption of the DBT molecule. One mode corresponds to the formation of a sigma bond between the metal center and the sulfur atom. Such structures are well known in the area of organometallic chemistry and calculations suggested that the angle between the metal sulfur bond and the plane of the aromatic ring is about  $120^\circ$  (30–33). This mode of adsorption is generally believed to result in HDS reaction. When applied to  $\text{MoS}_2$  this mode of adsorption leads to various geometric arrangements. However, most of these arrangements require that the layer is isolated and cannot be obtained if the layers are stacked. For a stacked layer, only a pseudovertical geometry is possible and requires that three adjacent Mo ions are coordinatively unsaturated. These simple geometric considerations indicate that the vertical mode of adsorp-

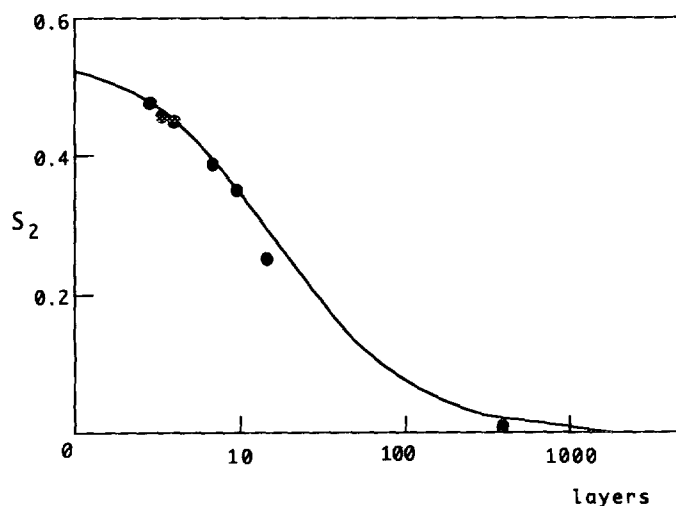


FIG. 14. Modeling of the variation of  $S_2$  with stacking.

tion is likely to be the mode resulting in the formation of the biphenyl. Note also that corners and edges should have a similar behavior. When considering an adsorption mode through the aromatic ring ( $\eta^6$  coordination for example), the situation is more complex. The mode which is likely to result in a hydrogenation reaction is the mode that covers the larger area of the catalyst surface. If the molecule binds so that it is parallel to the edge of the layer, it is clear that two other Mo ions will strongly interact with the molecule. It is unlikely that such geometry will be allowed on edge sites. One exception to this is found for the corner site, since the part of the molecule which is not bonded to the Mo center will be hanging in space. If the molecule binds so that it is orthogonal to the edge of the layer, no additional interactions with the binding layer occurs, but the neighboring layer if it exists will forbid such geometry. This implies that only single layers or the top and bottom layers of a stack would allow the hydrogenation reaction to occur because they are the only layer that are not sandwiched. A convenient model of DBT adsorption on an MoS<sub>2</sub> particle has been described by Daage and Murray (34).

We summarize the above arguments by saying that for small molecules previous corner edge models may be sufficient to describe HDS selectivity on MoS<sub>2</sub> catalysts. However, for larger molecules steric factors come into play and the interference of adjacent layers results in a sterically based selectivity, dependent on the stack height of the MoS<sub>2</sub>. We further note that the model presented does not predict 100% hydrogenation for single layers but something approaching 60% under conditions used in this study. Thus, previous corner/edge models may become coincident with the rim/edge model presented here. Indeed, as mentioned above most studies were on low-stack materials.

It is also possible to imagine that the stack height dependence outlined in this report is related to some relation between the crystallization in the stack direction and ordering of the edge site. We believe that this is a more complex model and that the data support the simpler model presented. In order to obtain the correlations observed the ratio of corners to edge should vary as  $1/n$  in a regular manner. Although mathematically possible, we consider this possibility unlikely. If this were so, we should expect that the corner to edge ratio would rather follow the increase in crystallinity within the basal plane direction, which it does not. This might occur on stepped surfaces corresponding to low density planes, which are relatively unstable. One possible structure is the (2110) plane which has a surface energy that is 15% higher than that of the (1010) plane (35). Such planes have been observed by microdiffraction in supported MoS<sub>2</sub> catalysts. These structures were found on certain particles where

there was an obstacle to growth (36). These particles were bonded edge up and the existence of the (2110) plane was attributed to a stabilization by the (110) plane of the alumina. This suggests that the stepped surfaces are quite unstable and that the ratio of corner to edge in a given layer is rather low.

As discussed above corner sites are also present but, for the large MoS<sub>2</sub> particles reported here, it is likely that the concentration of rim sites is much larger than the concentration of corner sites, particularly when the stacking is low. Nevertheless, the wonderful complexity and versatility of these catalysts still continue to challenge the researcher and present new surprises.

## CONCLUSIONS

We have shown that the catalytic activity of unsupported molybdenum sulfide is related to the coexistence of two different sites as previously reported. However, the relative concentrations of these sites are directly dependent upon the morphology of the MoS<sub>2</sub> crystallites and more precisely upon the stacking height of the layers which can be easily estimated by X-ray diffraction. Hydrogenation reaction is found to be catalyzed predominantly by rim sites for large molecules like DBT. Sulfur removal is catalyzed by edge sites. Turnover frequencies are reported for all major products and selectivity functions are presented which allow prediction of the product under the conditions reported, based only on the turnover numbers and the stack height of the MoS<sub>2</sub>.

The selectivity model presented arises because of steric hinderance which occurs when DBT is adsorbed on an edge site, the adjacent layers interfering with the adsorption. This interference does not occur on the rim sites allowing more hydrogenation mode adsorption. When single layers occur, selectivity is dominated by the degree of coordinative unsaturation present. Smaller sulfur-containing molecules may not exhibit the rim/edge effect due to the absence of steric interference.

Future work will expand the role of steric influence in HDS, an effect which should have important consequences as petroleum feedstocks contain more, heavier sulfur-bearing molecules. Also, left to a future report is the role of promoters such as Co and Ni which is not addressed in this report.

## ACKNOWLEDGMENTS

The authors thank Dr. T. R. Halbert for valuable discussions, R. Krycak for operating the reactor unit, and C. R. Symon for the preparation of the catalysts.

## REFERENCES

1. Chianelli, R. R., *Catal. Rev. Sci. Eng.* **26**, 361 (1984).
2. Ratnasamy, P. and Sivasanker, S., *Catal. Rev. Sci. Eng.* **22**, 401 (1980).
3. Voorhoeve, R. J. H., and Stuver, J. C. M., *J. Catal.* **23**, 228, 243 (1971).
4. Farragher, A. L., and Cossee, P., "Proceedings, 5th International Congress on Catalysis, Palm Beach, 1972" (J. W. Hightower, Ed.), North-Holland, Amsterdam, 1973.
5. Tauster, S., Pecoraro, T. A., and Chianelli, R. R., *J. Catal.* **63**, 515 (1980).
6. Silbernagel, B. G., Pecoraro, T. A., and Chianelli, R. R., *J. Catal.* **78**, 380 (1982).
7. Johnston, D. C., Silbernagel, B. G., Daage, M., and Chianelli, R. R., "Proceedings, 189th ACS National Meeting, Miami, 1985, paper PETR 76.
8. Tanaka, K. I., *Adv. Catal.* **33**, 99 (1985).
9. Okuhara, T., and Tanaka, K. I., *J. Phys. Chem.* **82**, 1953 (1978).
10. Chianelli, R. R., Ruppert, A. F., Behal, S. K., Wold, A., and Kershaw, R., *J. Catal.* **92**, 56 (1985).
11. Chianelli, R. R., *Int. Rev. Phys. Chem.* **2**, 127 (1982).
12. Tanaka, K. I., and Okuhara, T., *Catal. Rev. Sci. Eng.* **15**, 249 (1977).
13. Roxlo, C. B., Daage, M., Ruppert, A. F., and Chianelli, R. R., *J. Catal.* **100**, 176 (1986).
14. Massoth, F. E., *Adv. Catal.* **27**, 265 (1978).
15. Delmon, B., "Proceedings, Climax 3rd International Conference on Chemistry and Uses of Molybdenum," 1979. (H. F. Barry and P. C. H. Mitchell, Eds.).
16. Ratnasamy, P., and Sivasanker, S., *Catal. Rev. Sci. Eng.* **22**, 401 (1980).
17. Topsøe, H., Clausen, B. S., Candia, R., Wivel, C., and Morup, S. J., *J. Catal.* **68**, 433 (1981).
18. Muralidhar, G., Massoth, F. E., and Shabtai, J., *ACS Div. Pet. Chem. Prep.* **27**, 722 (1982).
19. Kasztelan, S., Toulhouat, H., Grimblot, J., and Bonnelle, J. P., *Appl. Catal.* **13**, 127 (1984).
20. Kaszelan, S., *Langmuir* **6**, 590 (1990).
21. Wambeke, A., Jalowiecki, L., Kasztelan, S., Grimblot, J., and Bonnelle, J. P., *J. Catal.* **109**, 319 (1988).
22. Kasztelan, S., Jalowiecki, L., Wambeke, A., Grimblot, J., and Bonnelle, J. P., *Bull. Soc. Chim. Belg.* **96**, 1003 (1987).
23. Roxlo, C. B., Deckman, H. W., Gland, J., Cameron, S. D., and Chianelli, R. R., *Science* **235**, 1629 (1987).
24. Singhal, G. H., Espino, R. E., Sobel, J. E., and Huff, G. A., *J. Catal.* **67**, 457 (1981).
25. Broderick, D. H., and Gates, B. C., *AIChE J* **27**, 663 (1981).
26. Vrinat, M. L., *Appl. Catal.* **6**, 137 (1983).
27. Press, W. H., Teukosky, S. A., Vetterling, W. T., and Flannery, B. P., in "Numerical Recipes in Fortran" 2nd ed., p. 702. Cambridge Univ. Press, 1992.
28. Tanaka, K. I., and Okuhara, T., "Proceedings, 3rd International Conference on the Chemistry and Uses of Molybdenum," p. 170, Ann Arbor Michigan, August 19-23, 1979.
29. Kemp, R. A., Ryan, R. C., and Smegal, J. A., "Proceedings, 9th International Congress on Catalysis, Calgary, 1988" (M. J. Phillips and M. Ternan, Eds.), Chem. Institute of Canada, Ottawa, 1988.
30. Angelici, R. J., *Coord. Chem. Rev.* **105**, 61 (1990).
31. Rauchfuss, T. B., *Prog. Inorg. Chem.* **39**, 259 (1991).
32. Jones, W. D., and Chin, R. M., *J. Am. Chem. Soc.* **114**, 9851 (1992).
33. Sakugset, A. E., Rauchfuss, T. B., and Wilson, S. R., *J. Am. Chem. Soc.* **114**, 8521 (1992).
34. Daage, M., and Murray, H. H., in "Preprints of the 1st Symposium on Advances in Hydrotreating," sponsored by the Petroleum Division of the ACS, August 22-27, 1993, Chicago.
35. Hayden, T. F., Ph.D. dissertation, University of Wisconsin-Madison, 1986.
36. Hayden, T. F., Dumesic, J. A., *J. Catal.* **103**, 366 (1987).